


 Cite this: *Chem. Commun.*, 2021, 57, 7681

 Received 21st May 2021,
Accepted 16th June 2021

DOI: 10.1039/d1cc02671b

rsc.li/chemcomm

Optically active covalent organic frameworks and hyperbranched polymers with chirality induced by circularly polarized light†

 Yuting Wang,^a Koji Yazawa,^b Qingyu Wang,^a Takunori Harada,^{ib} Shuhei Shimoda,^d Zhiyi Song,^a Masayoshi Bando,^a Naofumi Naga^e and Tamaki Nakano^{ib}*^{af}

Axial chirality was induced by circularly polarized light to covalent organic frameworks as well as hyperbranched polymers composed of benzene-1,3,5-triyl core units and oligo(benzene-1,4-diyl) as linker units where variation in induction efficiency was rationally interpreted in terms of internal rotation dynamics studied through CPMAS ¹³C NMR experiments including CODEX measurements.

Chiral polymers are an important class of materials because of their wide scope of applications.^{1,2} While most studies have targeted linear polymers with a single-handed helical conformation controlled by chiral monomeric units or by catalysis or by external stimuli, chiral dendrimers and hyperbranched polymers (HBPs) composed of chiral units have also been reported.³ In addition, as newer chiral polymers with branching, covalent organic frameworks (COFs) have been drawing attention.^{4,5} The chiroptical properties of COFs arise mostly from chiral constituent units except in a case where an optically active small molecule induced chirality.⁶ With such a background, we herein report the preparation of optically active COFs and HBPs composed of benzene-1,3,5-triyl core and oligo(benzene-1,4-diyl) linker units having preferred-handed axial chirality (twist) around the benzene–benzene junctions induced by circularly polarized light (CPL). Preparation of optically active COFs and HBPs based on chirality of light has been unprecedented.

Chirality induction by CPL has been realized for linear polyfluorene derivatives and other small molecules having aromatic–aromatic (Ar–Ar) single bonds through enantiomer-selective excitation of axially chiral Ar–Ar units.^{7–11} Biphenyl as the simplest Ar–Ar compound has a twisted conformation in the ground state and is transformed to a coplanar conformation in excited states (twisted-coplanar transition),^{12,13} and if one of the enantiomeric twists is preferentially excited by CPL, the population of the un-excited twist increases, which leads to an optically active product (twist-sense-selective excitation).^{7–11,13–15} In this work, this methodology was applied for the COFs and HBPs composed of benzene–benzene junctions. CPL-based chirality induction has been reported also for other types of polymers.^{16,17}

Suzuki–Miyaura cross coupling reactions of the core monomer (C) with a linker monomer (L), namely, the reactions of 1,3,5-tribromobenzene with 1,4-bis(dihydroxyboranyl)benzene, 1,3,5-tribromobenzene with 4,4′-bis(dihydroxyboranyl)-1,1′-biphenyl, and 1,3,5-tris(4,4,5,5-tetramethyl-1,3,2-dioxaborolan-2-yl)benzene with 4,4′-dibromo-1,1′:4′,1′′-terphenyl led to poly(benzene-1,3,5-triyl-*alt*-benzene-1,4-diyl) [poly(Bz135-*alt*-Bz14)], poly(benzene-1,3,5-triyl-*alt*-1,1′-biphenyl-4,4′-diyl) [poly(Bz135-*alt*-BP44′)], and poly(benzene-1,3,5-triyl-*alt*-1,1′:4′,1′′-terphenyl-4,4′′-diyl) [poly(Bz135-*alt*-TP44′′)], respectively, at different [L]/[C] ratios (Scheme 1).^{18–20}

The polymerization products were composed of a tetrahydrofuran-(THF)-soluble part having a network structure (COF) and THF-soluble part having no cross linking (HBP) (Tables S1–S3 in the ESI†). The apparent averaged molar masses of the HBPs were less than about 1×10^3 (SEC, *vs.* polystyrene) while selected samples indicated mean diameters of *ca.* 16–80 nm in dynamic light scattering measurements (Fig. S14 in the ESI†).

The three COFs were irradiated with CPL in fine powder form sandwiched between two quartz, and poly(Bz135-*alt*-TP44′′) COF exhibited intense and clear CD spectra. The spectra obtained on L- and R-CPL irradiation were almost mirror images (Fig. 1A and Fig. S17 in the ESI†), indicating that the preferred-handed twist conformation was induced to benzene–benzene junctions

^a Institute for Catalysis (ICAT) and Graduate School of Chemical Sciences and Engineering, Hokkaido University, N21W10, Kita-ku, Sapporo 001-0021, Japan.
E-mail: tamaki.nakano@cat.hokudai.ac.jp

^b JEOL RESONANCE Inc., 3-1-2 Musashino, Akishima, Tokyo 196-8558, Japan

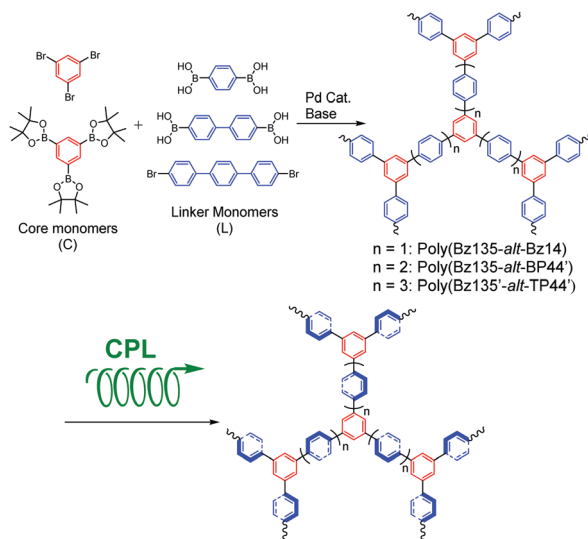
^c Department of Integrated Science and Technology, Faculty of Science and Technology, Oita University, Dannoharu, 700, Oita 870-1192, Japan

^d Technical Division, Institute for Catalysis, Hokkaido University, N21W10, Kita-ku, Sapporo 001-0021, Japan

^e Department of Applied Chemistry, College of Engineering, Shibaura Institute of Technology, 3-7-5 Toyosu, Koto-ku, Tokyo 135-8548, Japan

^f Integrated Research Consortium on Chemical Sciences (IRCCS), ICAT, Hokkaido University, Sapporo 001-0021, Japan

† Electronic supplementary information (ESI) available. See DOI: 10.1039/d1cc02671b



Scheme 1 Synthesis of COFs and HBPs composed of benzene rings and chirality induction of them by CPL.

through twist-sense-selective excitation. The chemical structure of the COF was found to be intact through CPL irradiation by IR spectra (Fig. S10 in the ESI†). In addition, the induced chirality was stable over months at ambient temperature.

The evolution in g_{CD} spectra was accompanied by a decrease in absorbance spectral intensity (Fig. S19 and S20 in the ESI†). This observation is ascribed to a change in the average dihedral angle around single bonds which has been clarified for biphenyl molecules by combined theoretical and experimental studies.²¹

CD intensity is discussed in terms of the Kuhn's anisotropy factor [$g_{\text{CD}} = 2(\epsilon_{\text{L}} - \epsilon_{\text{R}})/(\epsilon_{\text{R}} + \epsilon_{\text{L}})$ where ϵ_{L} and ϵ_{R} are molar absorptivities toward left-handed and right-handed CPL's, respectively]²² to eliminate the influence of absorbance intensity. Fig. 1B shows the plots of g_{CD} observed on L-CPL irradiation against relative irradiation energy sum at 326 nm whose definition is found in the ESI†. The g_{CD} -vs.-energy sum plot does not show a first-order type relation (an increasing form of exponential decay), and the early-stage data can be well

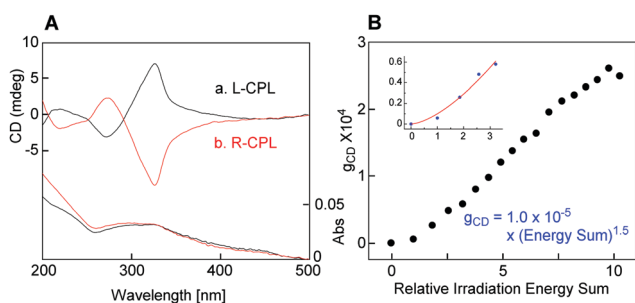


Fig. 1 CD-UV spectra of poly(Bz135-*alt*-TP44') COF (run 3 in Table S3-2 in the ESI†) observed on L-CPL (a) and R-CPL (b) irradiation [A] and g_{CD} -vs.-relative irradiation energy sum plots with curve fitting results (inset plots and corresponding equation) [B]. Maximum g_{CD} was $+2.5 \times 10^{-4}$ at 326 nm.

approximated with the power function indicated within Fig. 1B. Furthermore, the maximum g_{CD} of $+2.5 \times 10^{-4}$ at 326 nm after saturation of CD intensity upon L-CPL irradiation was much higher than expected for aromatic compounds on the basis solely of CPL chirality. Aromatic compounds at 100% ee generally show g_{CD} values of 10^{-3} to 10^{-4} order,^{13,23} and g_{CD} values attainable based only on CPL without amplification are of 10^{-6} to 10^{-8} order because the maximum ee values (γ_{PSS}) attainable at the photo stationary state follow the equation, $\gamma_{\text{PSS}} = 1/2 g_{\text{CD}(100\%ee)} \times 100\%$, which leads to maximum g_{CD} values decided by the equation, $g_{\text{CD}} = 1/100 \times \gamma_{\text{PSS}} \times g_{\text{CD}(100\%ee)} = 1/2 (g_{\text{CD}(100\%ee)})$.^{2,13,24} These results suggest that efficient chirality amplification took place through CPL irradiation of the COF.

On the other hand, poly(Bz135-*alt*-BP44') COF showed much weaker CD spectra, and poly(Bz135-*alt*-Bz14) COF did not respond to CPL irradiation (Fig. S17 in the ESI†). Regarding the differences among the three COFs, the three COFs showed rather similar transmission electron microscopy (TEM) images without any particularly regular structures (Fig. 2A, Fig. S15 in ESI†) while poly(Bz135-*alt*-Bz14) COF showed clear electron diffraction (ED) spots and the other two COFs did not (Fig. 2B, Fig. S15 in ESI†). On the other hand, none of the three COFs showed any diffraction patterns indicating molecular ordering in XRD measurements (Fig. S16 in the ESI†). These results may mean that poly(Bz135-*alt*-Bz14) COF has a short-distance ordered packing of benzene rings detected by ED but not by XRD. CPL irradiation may not induce effective rotation for poly(Bz135-*alt*-Bz14) COF due to a rigid structural order.

Furthermore, solid-state NMR analyses were conducted to probe the twisting motion in the COFs. The ¹³C CPMAS spectra of the COFs (Fig. 3A) showed two main signals of benzene rings corresponding to "C4" having no hydrogens and to "C3" having hydrogens at around 140 ppm and 127 ppm, respectively. The three spectra showed slightly different patterns which may reflect the difference in chemical structure among the three COFs.

To investigate the twisting motion, we first investigated the ¹³C longitudinal relaxation time in rotating frame ($T_{1\rho\text{C}}$) measurements which is sensitive to kHz order molecular motion. Three COFs indicated clear dependence of $T_{1\rho\text{C}}$ on the structure (Fig. S6 in the ESI†). The decay profiles of the C3 signals were well fitted with double exponential functions leading to shorter and longer relaxation times ($T_{1\rho\text{C}}^{\text{fast}}$, $T_{1\rho\text{C}}^{\text{slow}}$) while

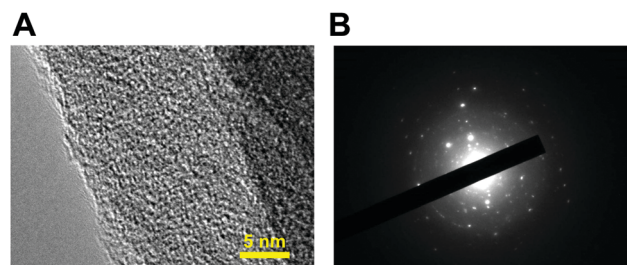


Fig. 2 TEM image (A) and electron diffraction profile (B) of poly(Bz135-*alt*-Bz14) COF (run 4 in Table S1 in the ESI†).

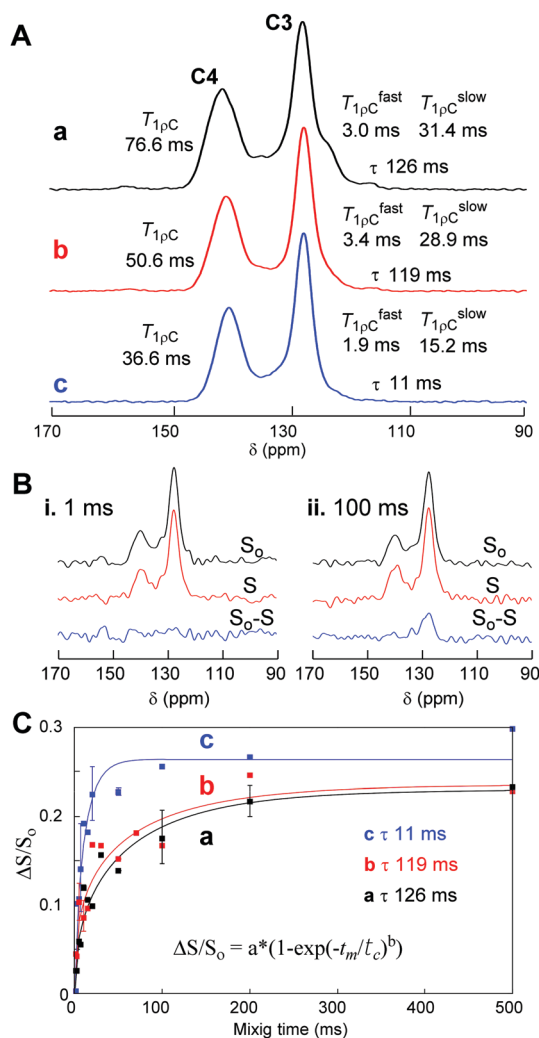


Fig. 3 ^{13}C CPMAS NMR spectra of poly(Bz135-*alt*-Bz14) COF (run 4 in Table S1 in the ESI †) (a), poly(Bz135-*alt*-BP44') COF (run 3 in Table S2, ESI †) (b), and poly(Bz135-*alt*-TP44'') COF (run 3 in Table S3-2 in the ESI †) (c) [A], ^{13}C CODEX spectra of poly(Bz135-*alt*-TP44'') COF with mixing time of 1 ms (i) and 100 ms (ii) including reference spectra (top), CODEX exchange spectra (middle), and pure exchange spectra (bottom) [B], and normalized pure exchange CODEX intensity of the C3 signals as a function of mixing time for poly(Bz135-*alt*-Bz14) COF (a), poly(Bz135-*alt*-BP44') COF (b), and poly(Bz135-*alt*-TP44'') COF (c) [C]. The fit curve in C is a stretched exponential $a*(1 - \exp(t_m/\tau_c)^b)$.

those of the C4 signals were well fitted with single exponential functions leading to one relaxation time ($T_{1\rho\text{C}}$) (Fig. S7–S9 in the ESI †). Considering that the C3 signals arise from the carbons at the 2- and 3-positions of the benzene-1,4-diyl “linker” units and those at the 2-, 4-, and 6-positions of the benzene-1,3,5-triyl “core” units, $T_{1\rho\text{C}}^{\text{fast}}$ and $T_{1\rho\text{C}}^{\text{slow}}$ probably reflect molecular motions of the former and the latter, respectively. The most plausible motion contributing to $T_{1\rho\text{C}}^{\text{fast}}$ is twisting (flipping) of the benzene-1,4-diyl units around the chirality axes, and it was shorter for poly(Bz135-*alt*-TP44'') COF (1.9 ms) than for the other two COFs showing similar values (3.4 ms, 3.0 ms), indicating that the small-angle twisting motion is faster for the

former COF than the other two. $T_{1\rho\text{C}}^{\text{slow}}$ of C3 and $T_{1\rho\text{C}}$ of C4 may reflect motions of the relevant carbons other than rotation including changes in their relative orientation within the COF structures which could occur in association with the rotation.

More direct motional information was obtained by “center band only detection exchange” (CODEX) NMR experiments.²⁵ The CODEX experiment detects slow molecular dynamics resulting from changes in the orientation dependent chemical shift frequencies during the mixing time, t_m . The C3 signals exhibited a pure exchange signal at a sufficient mixing time (100 ms) which was not confirmed for the C4 signals (Fig. 3B). This is direct evidence of reorientation of phenylene flip, namely the twisting motion. The correlation time (τ_c), which reflects molecular motion during mixing time, for C3 was estimated from the pure exchange intensity as a function of t_m (Fig. 3C).^{25,26} The obtained τ_c for poly(Bz135-*alt*-TP44'') COF (11 ms) was much shorter than for the other two COFs showing similar values (119 ms, 121 ms), indicating that the twisting motion of benzene-1,4-diyl units occurs much smoother in poly(Bz135-*alt*-TP44'') COF than in the other two COFs. It has been reported that rotation of benzene-1,4-diyl units in linear poly(benzene-1,4-diyl-*alt*-ethene-1,2-diyl) occurs in the millisecond time scale ($\tau_c = 10$ ms).²⁵ The twisting motion in poly(Bz135-*alt*-TP44'') COF may occur at a similar rate.

The observations discussed so far suggest that the rotation around the chirality axes was much more smoothly activated by photo excitation in poly(Bz135-*alt*-TP44'') COF than in the other two in which greater steric crowdedness inside the frameworks can hamper such a motion. The density of branching points (core units) thus sensitively affects the freedom of inner rotation in the COFs.

Soluble HBPs were also subjected to CPL irradiation in solution-cast film (Fig. 4). All three HBPs exhibited clear, mirror-image CD spectra upon L- and R-CPL excitation where the chemical structures were found intact by IR spectra (Fig. S11 in the ESI †), indicating that CPL has introduced a preferred-handed twisted conformation.

The maximum g_{CD} values were much greater than those expected based only on CPL chirality, and the early-stage data in the g_{CD} -vs.-relative irradiation energy sum plots were well approximated with the power functions shown in Fig. 4, suggestive of chirality amplification. The chirality induction efficiency was rather similar among the three HBPs while the maximum g_{CD} value and the exponent of the power function were slightly greater for the poly(Bz135-*alt*-Bz14) HBP than the other two, which may mean that the higher branching density in the poly(Bz135-*alt*-Bz14) HBP is advantageous in chirality induction, which was not the case for the COFs.

The sharp contrast in chirality induction between the COFs and the HBPs having the same chemical structures may mean that the COFs have a much more rigid structure based on the extended network than HBPs, and the rotation motion is much more restricted in the COFs. This is supported by the fact that a longer irradiation time was necessary for poly(Bz135-*alt*-TP44'') (up to 45 min) than for the HBPs (up to 10 min) to complete chirality induction.

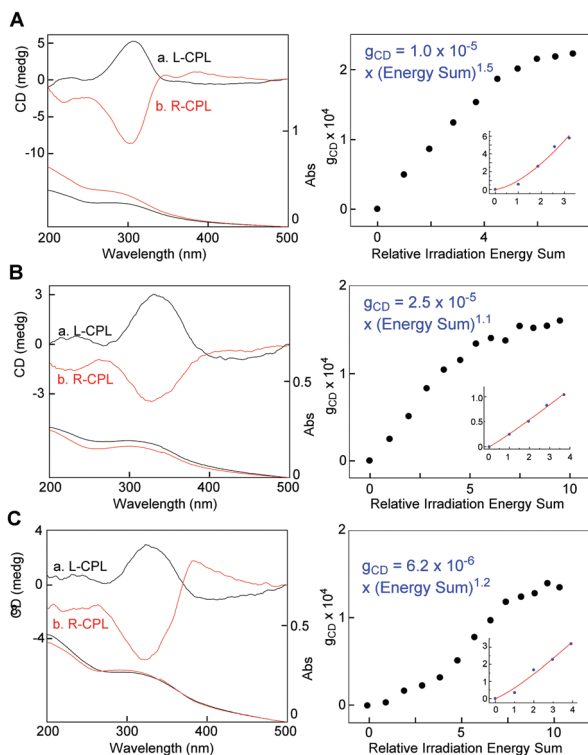


Fig. 4 CD-UV spectra observed on L-CPL (a) and R-CPL (b) irradiation [left] and g_{CD} -vs.-relative irradiation energy sum plots with curve fitting results (inset plots and corresponding equation) [right] of poly(Bz135-alt-Bz14) HBP (run 4 in Table S1 in the ESI†) (A), poly(Bz135-alt-BP44') HBP (run 3 in Table S2 in the ESI†) (B), and poly(Bz135-alt-TP44'') HBP (run 3 in Table S3-2 in the ESI†) (C). Maximum g_{CD} was $+2.2 \times 10^{-4}$ at 308 nm (A), $+1.6 \times 10^{-4}$ at 331 nm (B), and $+1.4 \times 10^{-4}$ at 323 nm (C).

Also, it is notable that chirality was efficiently induced for the amorphous HBPs because ordered structures enhancing intermolecular interactions have been found crucial in CPL-based chirality induction in both linear polymer and small-molecular systems so far studied.^{10–12} Strong enough intramolecular interactions may be realized even in the amorphous structure of HBPs due to the branched architecture.

In conclusion, chirality was successfully induced to poly(Bz135-alt-TP44'') COF and the three HBPs, and the distinctive responses to CPL irradiation of the three COFs were rationally understood in terms of the rate of internal rotation estimated by the CODEX NMR experiments. For the COFs, the chirality induction efficiency was higher when the linker unit was longer as a shorter linker may not allow smooth rotation around the chirality axes. Chirality induction to the HBPs was smoother than to the COFs, which may reflect the difference in structural rigidity between the HBPs and the COFs. While there have been various reports of chirality induction using CPL, details of the induced chiral structures and mechanistic features still appear to need further clarification, especially for the examples dealing with polymers in the solid state. The present studies using a series of COFs and HBPs composed of benzene-benzene junctions having systematically altered chemical structures and including a view of conformational

dynamics may provide deeper insights into the molecular mechanisms of chirality induction by light. Furthermore, the facile preparation of chiral COFs and HBPs using CPL may lead to development of novel optically active, solid-state materials with branching showing various chiral functions.

This work was supported in part by the MEXT/JSPS KAKENHI Grant Number JP 19H02759 and in part by the JST grant No. JPM1JT19E4. The Technical Division of Institute for Catalysis, Hokkaido University is acknowledged for technical support.

Conflicts of interest

There are no conflicts to declare.

Notes and references

- (a) E. Yashima, K. Maeda, H. Iida, Y. Furusho and K. Nagai, *Chem. Rev.*, 2009, **109**, 6102–6211; (b) E. Yashima, N. Ousaka, D. Taura, K. Shimomura, T. Ikai and K. Maeda, *Chem. Rev.*, 2016, **116**, 13752–13990.
- (a) T. Nakano and Y. Okamoto, *Chem. Rev.*, 2001, **101**, 4013–4038; (b) Y. Okamoto and T. Nakano, *Chem. Rev.*, 1994, **94**, 349–372.
- A.-M. Caminade, P. Servin, R. Laurent and J.-P. Majoral, *Chem. Soc. Rev.*, 2008, **37**, 56–67.
- X. Han, C. Yuan, B. Hou, L. Liu, H. Li, Y. Liu and Y. Cui, *Chem. Soc. Rev.*, 2020, **49**, 6248–6272.
- Z. Wang, S. Zhang, Y. Chen, Z. Zhang and S. Ma, *Chem. Soc. Rev.*, 2020, **49**, 708–735.
- X. Han, J. Zhang, J. Huang, X. Wu, D. Yuan, Y. Liu and Y. Cui, *Nat. Commun.*, 2018, **9**, 1–10.
- Y. Wang, T. Sakamoto and T. Nakano, *Chem. Commun.*, 2012, **48**, 1871–1873.
- Y. Wang, T. Harada, L. Q. Phuong, Y. Kanemitsu and T. Nakano, *Macromolecules*, 2018, **51**, 6865–6877.
- A. Pietropaolo, Y. Wang and T. Nakano, *Angew. Chem., Int. Ed.*, 2015, **127**, 2726–2730.
- Y. Wang, A. L. Kanibolotsky, P. J. Skabara and T. Nakano, *Chem. Commun.*, 2016, **52**, 1919–1922.
- Z. Zhang, T. Harada, A. Pietropaolo, Y. Wang, Y. Wang, X. Hu, X. He, H. Chen, Z. Song, M. Bando and T. Nakano, *Chem. Commun.*, 2021, **57**, 1794–1797.
- A. Imamura and R. Hoffmann, *J. Am. Chem. Soc.*, 1968, **90**, 5379–5385.
- T. Nakano, *Chem. Rec.*, 2014, **14**, 369–385.
- A. Pietropaolo and T. Nakano, *J. Am. Chem. Soc.*, 2013, **135**, 5509–5512.
- A. Pietropaolo and T. Nakano, *Chirality*, 2020, 1–6.
- L. Nikolova, T. Todorov, M. Ivanov, F. Andruzzi, S. Hvilsted and P. S. Ramanujam, *Opt. Mater.*, 1997, **8**, 255–258.
- L. Wang, L. Yin, W. Zhang, X. Zhu and M. Fujiki, *J. Am. Chem. Soc.*, 2017, **139**, 13218–13226.
- R. S. Sprick, B. Bonillo, M. Sachs, R. Clowes, J. R. Durrant, D. J. Adams and A. I. Cooper, *Chem. Commun.*, 2016, **52**, 10008–10011.
- Catherine M. Aitchison, R. S. Sprick and A. I. Cooper, *J. Mater. Chem. A*, 2019, **7**, 2490–2496.
- K. V. Rao, S. Mohapatra, C. Kulkarni, T. K. Maji and S. J. George, *J. Mater. Chem.*, 2011, **21**, 12958–12963.
- A. Pietropaolo, C. Cozza, Z. Zhang and T. Nakano, *Liq. Cryst.*, 2018, **45**, 2048–2053.
- W. Kuhn, *Trans. Faraday Soc.*, 1930, **26**, 293–308.
- Y. Inoue, *Chem. Rev.*, 1992, **92**, 741–770.
- J. Li, G. B. Schuster, K.-S. Cheon, M. M. Green and J. V. Selinger, *J. Am. Chem. Soc.*, 2000, **122**, 2603–2612.
- E. DeAzevedo, R. Franco, A. Marletta, R. Faria and T. Bonagamba, *J. Chem. Phys.*, 2003, **119**, 2923–2934.
- W. Hu, T. Bonagamba and K. Schmidt-Rohr, *J. Am. Chem. Soc.*, 1999, **121**, 8411–8412.